Frontiers in Power and Energy Systems (2025)
Clausius Scientific Press, Canada

DOI: 10.23977/fpes.2025.040105
ISSN 2516-2926 Vol. 4 Num. 1

Estimation Method for Membrane Water Content in Proton Exchange Membrane Fuel Cells

Su Zhou[1,a], Wenhao Guo[1,b], Keda Li[1,c], Jianhua Gao[2,d], Fenglai Pei[3,e,*]

[1]College of Automotive Studies, Tongji University, Shanghai, 201804, China
[2]Research Institute of Highway, Ministry of Transport, Beijing, 100088, China
[3]Shanghai Motor Vehicle Inspection Certification & Tech Innovation Center Co., Ltd., Shanghai, 201805, China
[a]suzhou@tongji.edu.cn, [b]2133569@tongji.edu.cn, [c]2133572@tongji.edu.cn, [d]gao.jh@rioh.cn, [e]fenglaip@smvic.com.cn
**Corresponding author*

Keywords: Fuel Cell; Membrane Water Content; Luenberger Observer; State Observer

Abstract: With the increasing demand for energy, proton exchange membrane fuel cell (PEMFC) is gradually being developed for high-power applications. The power output of a single fuel cell is limited, so multi-stack fuel cell systems (MFCS) are used to meet high-power demands. The performance of fuel cells is influenced by membrane water content, but since it cannot be directly measured by sensors, indirect methods are required for estimation. Although previous studies have used Luenberger observers to estimate the membrane water content of single-stack fuel cells, the air subsystem of multi-stack systems is more complex, with stronger variable coupling and nonlinearity, making single-stack methods difficult to apply directly. To address this, the study focuses on MFCS and derives membrane water content dynamics via mass conservation. A piecewise system identification approach yields state and input-output matrices near steady states. Observability is verified, and a Luenberger observer is designed for estimating membrane water content under varying power levels. Experiments show stable and accurate estimation, supporting MFCS health management and control.

1. Introduction

Hydrogen, the most abundant element in the universe, is considered an "inexhaustible and sustainable" energy source. Its light weight, high energy density, and cleanliness make it a promising "ultimate energy." Hydrogen fuel cells, with a the oretical efficiency of up to 90%[1], outperform traditional power generation devices and are key for zero-emission vehicles. A typical fuel cell system includes a fuel cell stack, air and hydrogen supply systems, and thermal management. However, due to technological complexity or measurement limitations, some internal variables, like membrane water content, are difficult to measure. Membrane hydration significantly affects proton conductivity and fuel cell performance. As Liu[2] noted that proper hydration improves proton conductivity, while a dry membrane reduces it, increasing ohmic losses. Therefore, estimating membrane water content is crucial for fuel cell monitoring and control.

Some researchers have explored real-time monitoring of internal humidity in fuel cells. For instance, Zhao[3] divided the cathode into nine sections and used micro humidity sensors, finding that cathode humidity significantly affects the polarization curve. However, limited internal space, high sensor costs, and response delays hinder practical application. Jiao et al. [4] developed an adaptive sliding mode observer to estimate humidity in both anode and cathode, showing reduced average estimation error in an 80 kW fuel cell. Yet, the method involves complex computations, strong model dependency, and sensitivity to parameter variations. Jian et al.[5] proposed a PEM humidity estimation approach based on interval type-2 fuzzy logic and the Cuckoo Search algorithm, achieving accurate nonlinear fitting but facing limitations due to high model complexity and computational demand. Zhu [6] used interval type-2 fuzzy logic for soft-sensing modeling of PEM humidity, benefiting from its nonlinear approximation capability. Hu[7] formulated a state estimation problem using a cathode two-phase dynamic model, designing a Luenberger observer and an unscented Kalman filter (UKF) to estimate liquid water content under flooding, but this approach also suffers from high complexity and computational cost.

To improve real-time monitoring of membrane water content while reducing model complexity and parameter tuning, this paper proposes a Luenberger observer-based method for estimating PEM water content in multi-stack fuel cell systems (MFCS). Unlike traditional methods, it uses mass conservation principles and piecewise system identification to derive system matrices, enhancing accuracy and stability. Observability analysis and an optimized feedback gain further ensure robustness under varying conditions. This approach simplifies modeling, supports multi-stack systems, and offers practical value, with both theoretical and real-world significance for fuel cell technology.

2. Multi-stack fuel cell system stack modelling

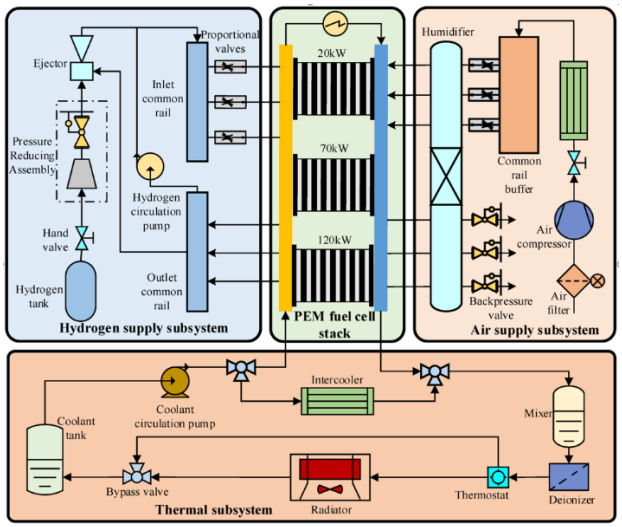

Figure 1: MFCS model structure.

The air subsystem of MFCS is complex, with numerous actuators and strongly coupled, nonlinear internal variables. To meet high power demands, this study adopts a multi-stack PEMFC system architecture. In such systems, power allocation strategies significantly impact overall performance. While the traditional equal distribution method is simple, it may reduce efficiency when stack performance varies. In contrast, stepwise allocation adjusts load dynamically based on metrics like efficiency and lifespan, making it suitable for high-performance applications. For example, Zhou et al.[8] developed a power management model for heavy-duty vehicles that optimizes stack allocation

based on efficiency and remaining useful life, using iterative and heuristic algorithms to determine optimal configurations for three to five stacks. Gao et al. [9] proposed an optimized stack allocation method considering both economics and dynamics (see Fig. 1), showing that MFCS systems with 20 kW, 70 kW, and 120 kW targets could meet both efficiency and lifespan requirements.

To cover typical applications from low to high power, this study adopts 20 kW, 70 kW, and 120 kW multi-stack architectures, based on the MFCS model proposed by Gao et al. [9]. A simplified model of the fuel cell stacks is developed. Since this work focuses on macro-level control, the effects of flow field geometry, gas diffusion layers, and catalyst layers are not considered. The stack model aims to describe gas consumption and production, membrane transport, heat exchange, and power output. It includes sub-models for the cathode and anode flow channels, membrane water transport, and stack voltage output, as shown in Fig. 2.

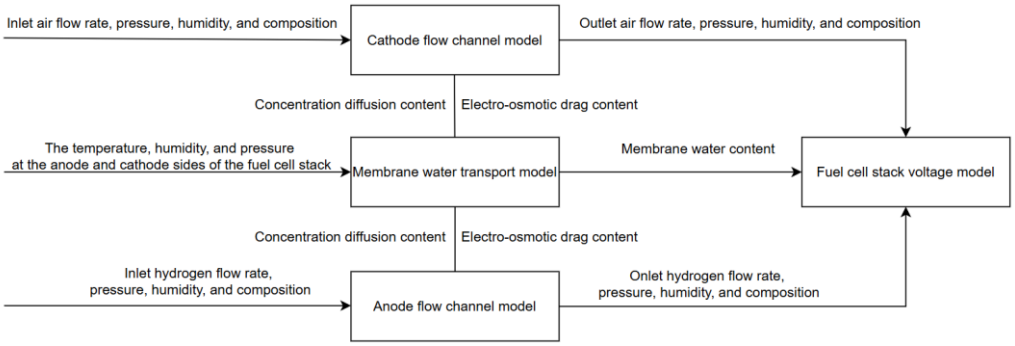

Figure 2: Stack model structure.

Some key parameters of the MFCS used in this study are shown in Table 1.

Table 1: Key Parameters of MFCS.

Parameter	Value	Parameter	Value
Number of Cells in Stack 1	120	Internal Temperature of Stack (℃)	75
Number of Cells in Stack 2	440	Density of Membrane when dry (kg/cm^3)	0.002
Number of Cells in Stack 3	630	Molar Mass of Membrane when dry (kg/mol)	1.1
Proton Exchange Membrane Area (cm^2)	120	Thickness of Proton Exchange Membrane (cm)	0.012

3. Membrane Water Content Estimation Method

According to the voltage equation of PEMFC, the output voltage is affected by the oxygen partial pressure. Therefore, conventional air system control strategies often consider the pressure and flow rate inside the stack. Under varying operating conditions, the inlet humidity of the stack is not constant. Since membrane water content directly impacts both efficiency and lifespan of the fuel cell, it is essential to incorporate control based on membrane hydration (i.e., a function related to humidity).

Membrane water content significantly affects fuel cell performance. Studies have shown that cathode humidity heavily influences output voltage and power density, with optimal performance typically achieved near 80% relative humidity. Yousefkhani et al. [10] reported an 8.5% increase in peak power density when cathode humidity rose from 50% to 80%, while Shi et al. [11] observed a 10% voltage rise at low current densities as humidity increased. These results suggest that maintaining cathode humidity around 80% is beneficial for maximizing fuel cell performance.

3.1. Humidity Estimation Algorithm

Fuel cells usually receive corresponding signals through sensors for pressure and flow control.

When using sensors to observe humidity, humidity has a large delay, that is, the sensor can only obtain the humidity at a historical moment. At the same time, humidity sensors are expensive and difficult to place inside a small fuel cell stack. Therefore, other methods are needed to indirectly obtain the humidity inside the fuel cell.

For linear time-invariant systems, a Luenberger state observer can be used. The basic principle is to estimate the internal states by correcting the system output feedback, ensuring that the estimated states converge to the actual states over time[12]. The structure is shown in Fig. 3.

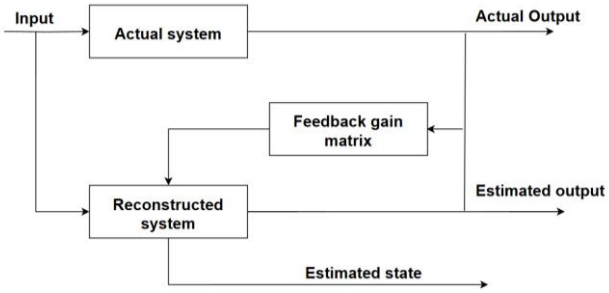

Figure 3: Structure diagram of the state observer.

The original system can be expressed as follows:

$$\begin{cases} \dot{x} = Ax + Bu \\ y = Cx \end{cases} \tag{1}$$

where x is the system state, defined as the cathode and anode humidity in this study, u is the input, and y is the output. A is the state transition matrix, B is the input matrix, and C is the output matrix.

The Luenberger observer reconstructs the system's (ABC) matrices with a feedback correction term to ensure estimated states converge to actual values. Its structure is given by:

$$\begin{cases} \dot{\hat{x}} = A\hat{x} + Bu + G(y - \hat{y}) \\ \hat{y} = C\hat{x} \end{cases} \tag{2}$$

where $\hat{x}$ is the estimated state, $\hat{y}$ is the estimated output, and G is the feedback gain matrix.

Let the error between the actual state and estimated state be e, then $\dot{e}$ can be expressed as:

$$\dot{e} = \dot{x} - \dot{\hat{x}} = A(x - \hat{x}) - G(y - \hat{y}) = (A - GC)e \tag{3}$$

If the real part of the eigenvalues of $A - GC$ is less than 0, the error eee will converge to 0 over time. That is, as time approaches infinity, the estimated state will approach the actual state.

3.2. Humidity State-Space Equations

To establish the state-space model for humidity dynamics, this study defines the system inputs, outputs, and state variables through humidity-influencing factor analysis. Key assumptions include: uniform water vapor distribution, constant 348K operating temperature, and negligible liquid water blockage effects. For a single stack, humidity depends on inlet vapor, electro-osmosis, back diffusion, and reaction-generated water.

(1) Incoming Stack Water Vapor

The cathode and anode inlet streams within the fuel cell carry water vapor that directly impacts membrane hydration. Their moisture contributions can be expressed as:

$$\dot{n}_{ca,H_2O,in} = \frac{\dot{n}_{ca,in}\varphi_{ca,in}P_{sat}}{P_{ca,in}}, \qquad \dot{n}_{an,H_2O,in} = \frac{0.4\dot{n}_{an,in}P_{sat}}{P_{an,in}} \tag{4}$$

In the equation, $\dot{n}_{ca}^{in}$is the cathode inlet molar flow rate, Z is the cathode inlet humidity, P_{ca}^{in} is the cathode inlet pressure, $\dot{n}_{an}^{in}$ is the anode inlet molar flow rate, P_{an}^{in} is the anode inlet pressure, and P_{sat} is the saturation vapor pressure at the current temperature. To simplify the estimation algorithm, the anode inlet relative humidity is assumed to be constant at 0.4.

(2) Electro-osmosis

Water is transferred from the anode to the cathode through electro-osmosis, which impacts the humidity at anode and cathode. The water content due to electro-osmosis can be expressed as:

$$\dot{n}_{H_2O,osm} = \frac{n_{cell} n_d I}{F} \tag{5}$$

where n_{cell} is the number of cells, I is the load current, and F is Faraday's constant, $n_d$is the electro-osmotic coefficient, given by:

$$n_d = 0.0029\lambda_m^2 + 0.05\lambda_m - 3.4 \times 10^{-19} \tag{6}$$

where λ_m is the membrane water content, expressed as:

$$\lambda_m = 0.043 + 17.81\left(\frac{\varphi_{ca} + \varphi_{an}}{2}\right) - 39.85\left(\frac{\varphi_{ca} + \varphi_{an}}{2}\right)^2 + 36\left(\frac{\varphi_{ca} + \varphi_{an}}{2}\right)^3 \tag{7}$$

where φ_{ca} is the cathode humidity and φ_{an} is the anode humidity.

(3) Concentration Diffusion

Due to the higher moisture content at the cathode compared to the anode, water diffuses from the cathode to the anode through the proton exchange membrane. This part typically transfers more water than electro-osmosis. The water content diffused can be expressed as:

$$\dot{n}_{H_2O,diff} = D_w \frac{c_{ca} - c_{an}}{l_m} \tag{8}$$

where D_w and c_{ca} are given by:

$$D_w = 10^{-6} A e^{2416\left(\frac{1}{303} - \frac{1}{T_{st}}\right)},\ c_{ca} = \frac{\rho_{m,dry}}{M_{m,dry}} \lambda_{ca} \tag{9}$$

where A is the area of the PEM, T_{st} is the stack temperature, $\rho_{m,dry}$ is the membrane's dry density, $M_{m,dry}$ is the membrane's molar mass in dry conditions, and λ_{ca} is the cathode water content.

(4) Reaction Water Generation

The water generated by the electrochemical reaction between hydrogen and oxygen is typically concentrated at the cathode. This water content can be expressed as:

$$\dot{n}_{ca,H_2O,gen} = \frac{n_{cell} I}{2F} \tag{10}$$

(5) Outgoing Water Vapor

The exhaust gases from the cathode and anode contain water vapor, which is recycled to the humidifier to humidify the incoming air. The water vapor content in the exhaust is given by:

$$\dot{n}_{ca,H_2O,out} = \frac{\dot{n}_{ca,out} \varphi_{ca} P_{sat}}{P_{ca}},\ \dot{n}_{an,H_2O,out} = \frac{\dot{n}_{an,out} \varphi_{an} P_{sat}}{P_{an}} \tag{11}$$

where $\dot{n}_{ca,out}$ is molar flow rate at cathode outlet, and $\dot{n}_{an,out}$ is molar flow rate at the anode outlet.

Based on ideal gas law, the humidity expressions for both cathode and anode can be derived as:

$$\begin{cases} \dot{\varphi}_{ca} = \dfrac{RT_{st}}{P_{sat}V_{ca}}\left(\dfrac{\dot{n}_{ca,in}\varphi_{ca,in}P_{sat}}{P_{ca,in}} + \dfrac{n_{cell}n_d I}{F} - D_w\dfrac{(c_{ca}-c_{an})}{l_m} + \dfrac{n_{cell}I}{2F} - \dfrac{\dot{n}_{ca,out}\varphi_{ca}P_{sat}}{P_{ca}}\right) \\ \dot{\varphi}_{an} = \dfrac{RT_{st}}{P_{sat}V_{an}}\left(\dfrac{0.4\dot{n}_{an,in}P_{sat}}{P_{an,in}} - \dfrac{n_{cell}n_d I}{F} + D_w\dfrac{(c_{ca}-c_{an})}{l_m} - \dfrac{\dot{n}_{an,out}\varphi_{an}P_{sat}}{P_{an}}\right) \end{cases} \tag{12}$$

where $\dot{\varphi}_{ca}$ and $\dot{\varphi}_{an}$ represent the change rates of cathode and anode humidity, respectively, and V_{ca} and V_{an} are the volumes of the cathode and anode channels.

From the above equations, it can be observed that the humidity at both the cathode and anode is influenced by inlet and outlet flow rates, pressure, load current, and other factors, and the relationships are highly nonlinear. These physical quantities change over time, and the variation patterns differ under different operating conditions. To generalize the humidity estimation algorithm and make it adaptable to various types of fuel cells and operating conditions, this study will use system identification methods, performing piecewise identification of the fuel cell system. The identified state transition, input, and output matrices will be used as the A, B, and C matrices for the state observer. The two state variables are cathode humidity and anode humidity, with the input being cathode inlet humidity, the disturbance input being load current, and the output being the fuel cell voltage.

3.3. System Output Equation

To design a Luenberger observer, a measurable output must be selected. Since the fuel cell voltage is directly measurable and influenced by anode/cathode humidity and membrane water content, it is chosen as the system output. The voltage can be expressed as a simplified nonlinear function of these humidity states and load current:

$$U = f(\varphi_{ca}, \varphi_{an}, I) \tag{13}$$

3.4. Nonlinear System Steady-State Point Selection

Since the fuel cell is a typical nonlinear system, and the Luenberger state observer is a full-dimensional linear observer, it can only be applied to linear systems. Therefore, a linearization approach for nonlinear systems is considered. It is approximated that the fuel cell exhibits good linearity around each operating point. Thus, near the equilibrium point, the original system can be written in the following incremental form:

$$\begin{cases} \Delta\dot{x} = A\Delta x + B\Delta u \\ \Delta y = C\Delta x \end{cases} \tag{14}$$

where A is the state transition matrix, B is the input matrix, and C is the output matrix. Δrepresents the deviation from the steady-state data.

Since the operating conditions and load currents vary, the CWTVC condition, which has the largest range of current demand, is used as an example for dividing the operating points, as shown in the fig. 4.

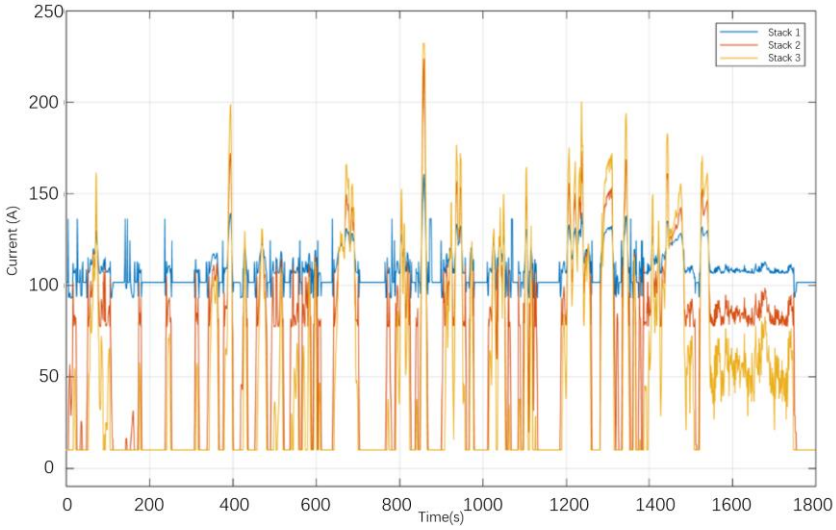

Figure 4: Variation of current in each stack under CWTVC operating conditions.

From Fig. 4, it can be seen that under the CWTVC condition, the required current for the three fuel cell stacks varies within the range of 10-230A. The steady-state operating conditions for the entire MFCS are summarized in Tab. 2 as shown below:

Table 2: Parameter calibration table of the fuel cell at different operating conditions.

	Point 1	Point 2	Point 3	Point 4
Current	28A	67.5A	115A	210A
Current Range	10-45A	45-85A	85-145A	145-230A
Cathode Humidity of Stack 1	62.5%	78.6%	92.9%	100%
Cathode Humidity of Stack 2	61.8%	75.4%	89.6%	100%
Cathode Humidity of Stack 3	63.7%	74.1%	91.7%	100%
Anode Humidity of Stack 1	70.3%	70.7%	72.2%	73.7%
Anode Humidity of Stack 2	80.5%	82.6%	84.2%	86.2%
Anode Humidity of Stack 3	80.4%	83.9%	85.5%	86.9%
Inlet Humidity of Stack 1	49.9%	60.3%	70.6%	81.6%
Inlet Humidity of Stack 2	48.3%	61.6%	69.4%	80.9%
Inlet Humidity of Stack 3	50.2%	59.7%	70.5%	82.2%
Voltage of Stack 1	105.1	95.9	92.6	88.1
Voltage of Stack 2	382.8	349	340.6	314.6
Voltage of Stack 3	549.7	503.8	494.1	457.8

3.5. System Identification

To enhance the adaptability of the humidity estimation algorithm, a system identification approach is used to construct the humidity observer. Since the same system identification method is applied to all three fuel cell stacks (20 kW, 70 kW, and 120 kW), this section uses the 20 kW stack as an example to describe the system identification process. The related processes for the 70 kW and 120 kW stacks are not elaborated here.

(1)Identification Signal Design

In this study, a step-like random signal is used as the identification signal to perform the system identification. The identification signal is shown in Fig. 5:

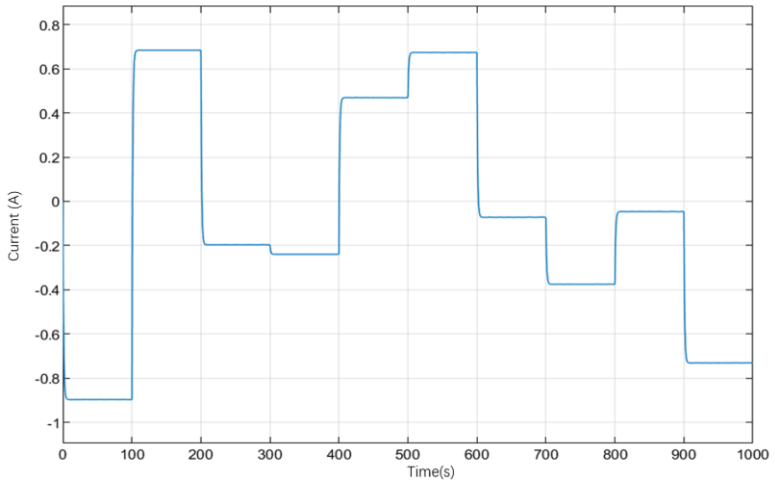

Figure 5: Diagram of the identification signal.

(2)Model Selection

Since the humidity observer contains two state variables and multiple inputs, and it can be assumed that, near each operating point, the variation of variables other than the anode and cathode humidity is negligible, a linear state-space model with an order of 2 is chosen for the identification model.

(3)Identification Process and Results

At four operating points, the system operates for 300 seconds to stabilize, after which the identification signal is injected into the original system and continuously excited for 1500 seconds to collect system output data. The input (cathode inlet humidity, load current) and output (fuel cell voltage) data are imported into the MATLAB identification toolbox to obtain identification results and accuracy at each operating point. The identification matrix for the 20 kW fuel cell stack is shown in Table 3:

Table 3: Identification matrix for the 20 kW stack.

Operating Point	A Matrix	B Matrix	C Matrix	Identification Accuracy
28A	$\begin{bmatrix}0.42 & -1.29\\ 9.06 & 2.75\end{bmatrix}$	$\begin{bmatrix}6.04e-4 & 0.06\\ -0.001 & -0.13\end{bmatrix}$	$[-11.87 \quad 0.28]$	0.82
67.5A	$\begin{bmatrix}-11.77 & -32.3\\ -7.41 & -23.8\end{bmatrix}$	$\begin{bmatrix}-6.06 & -6.06e+2\\ -4.23 & -4.24e+2\end{bmatrix}$	$[1.78 \quad -2.53]$	0.84
115A	$\begin{bmatrix}-3.19 & 5.51\\ -3.06 & 0.61\end{bmatrix}$	$\begin{bmatrix}5.51e-05 & 0.005\\ -4.75e-04 & -0.04\end{bmatrix}$	$[-0.17 \quad 2.56]$	0.76
210A	$\begin{bmatrix}-0.11 & 1.31\\ -0.92 & -15.25\end{bmatrix}$	$\begin{bmatrix}-3.96e-4 & -0.03\\ 0.004 & 0.44\end{bmatrix}$	$[17.6 \quad -1.27]$	0.88

3.6. Observability Test

Constructing a state observer requires the system to be observable—otherwise, a full-dimensional observer cannot estimate the system's state. Observability means the system's internal state can be determined from its measurable outputs and inputs. This paper uses the rank criterion to verify observability:

$$\begin{cases}\dot{x} = Ax + Bu\\ y = Cx\end{cases} \tag{15}$$

The necessary and sufficient condition for complete observability is that the rank of the observability matrix is full rank. The observability matrix can be expressed as:

$$s_0 = \begin{bmatrix} C \\ CA \\ \dots \\ CA^{n-1} \end{bmatrix} \tag{16}$$

For the MFCS in this paper, the observability matrix must be checked for full rank at each operating point. The observability matrix at each operating point is shown in Table 4:

Table 4: Rank of the observability matrix for the 20 kW stack.

Operating Point	Observability Matrix	Rank	Operating Point	Observability Matrix	Rank
28A	$\begin{bmatrix} -18.03 & -35.15 \\ 43.18 & -39.18 \end{bmatrix}$	2	115A	$\begin{bmatrix} -2.16 & -0.69 \\ -3.07 & 17.86 \end{bmatrix}$	2
67.5A	$\begin{bmatrix} 14.64 & -11.37 \\ -43.59 & -47.78 \end{bmatrix}$	2	210A	$\begin{bmatrix} -2.17 & 1.15 \\ 5.09 & 4.05 \end{bmatrix}$	2

As shown in Table 4, the observability matrix of the system is full rank at all operating points, indicating that the system is observable. Therefore, it is feasible to use a Luenberger state observer for full-dimensional state estimation.

3.7. Feedback Matrix Selection

The Luenberger observer's feedback matrix G must ensure $A - GC$ has negative eigenvalues for convergence, while avoiding excessive gain to prevent oscillations. In this work, pole placement and iterative tuning are used to set all eigenvalues of $A - GC$ to -10 across operating points. The resulting G matrices are listed in Table 5:

Table 5: Feedback matrix for the 20 kW stack.

Operating Point	Feedback Matrix G	Operating Point	Observability Matrix
28A	$[139.1808 \ -76.9369]$	115A	$[-75.9484;\ 44.3789]$
67.5A	$[-59.9701;\ -93.4093]$	210A	$[580.9;\ 1256.6]$

3.8. Incremental State Observer Construction

Using the incremental values of the anode and cathode humidity and their steady-state values as state variables, the incremental values of the cathode inlet humidity and load current as inputs, and the incremental values of the fuel cell voltage and steady-state values as outputs, the system is corrected through feedback to make the estimated states converge to the actual states. For each steady-state operating point, the entire incremental state observer model can be expressed as:

$$\begin{cases} \Delta\dot{\hat{x}} = A\Delta\hat{x} + B\Delta u + G(\Delta \mathrm{y} - \Delta\hat{y}) \\ \Delta\hat{\mathrm{y}} = \mathrm{C}\Delta\hat{x} \end{cases} \tag{17}$$

Where Δ represents the deviation from the steady-state values for each physical quantity, u is the actual input, and y is the actual output.

4. Humidity Estimation and Membrane Water Content Estimation Results

In this paper, the actual humidity is calculated using a mathematical model based on mass conservation and the ideal gas law, while the estimated humidity is derived from the observer. A comparison between the actual and estimated humidity is made to verify the reasonableness and accuracy of the humidity estimation algorithm.

Under the CWTVC operating condition, the changes in actual and estimated humidity for the

MFCS are shown in the following figures:

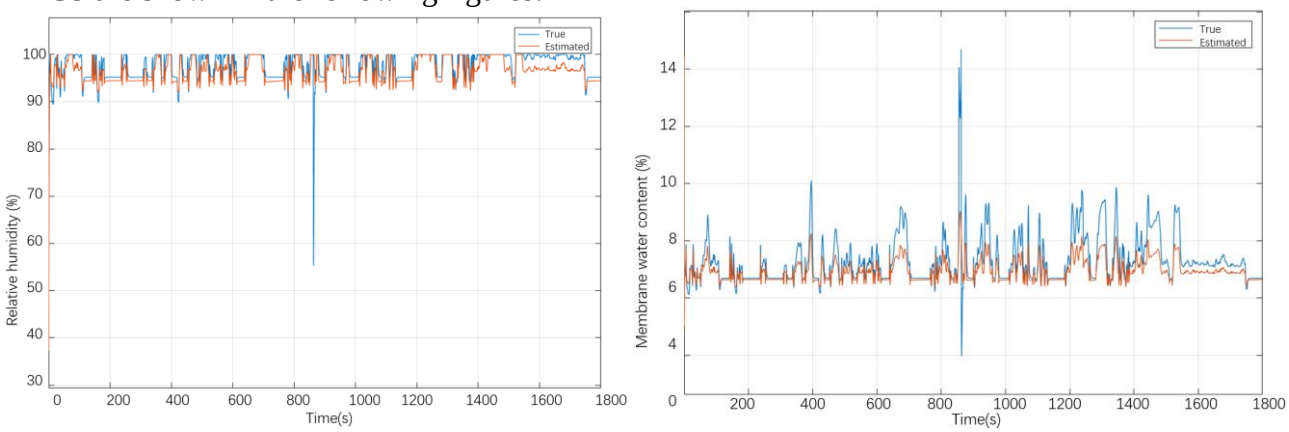

(a) (b)

Figure 6: Estimated vs. real humidity (a) and membrane water content (b) in the 20 kW stack.

As shown in Fig. 6, under the entire operating condition, the estimated humidity from the humidity observer for the 20 kW stack closely follows the trend of the actual humidity obtained through the mechanistic model. However, at 870 seconds, there is a noticeable jump in the estimated humidity. This is due to the fact that the load current of the stack reached the switching threshold at this point, causing the observer to switch its internal model, which resulted in the sudden change in the estimated humidity.

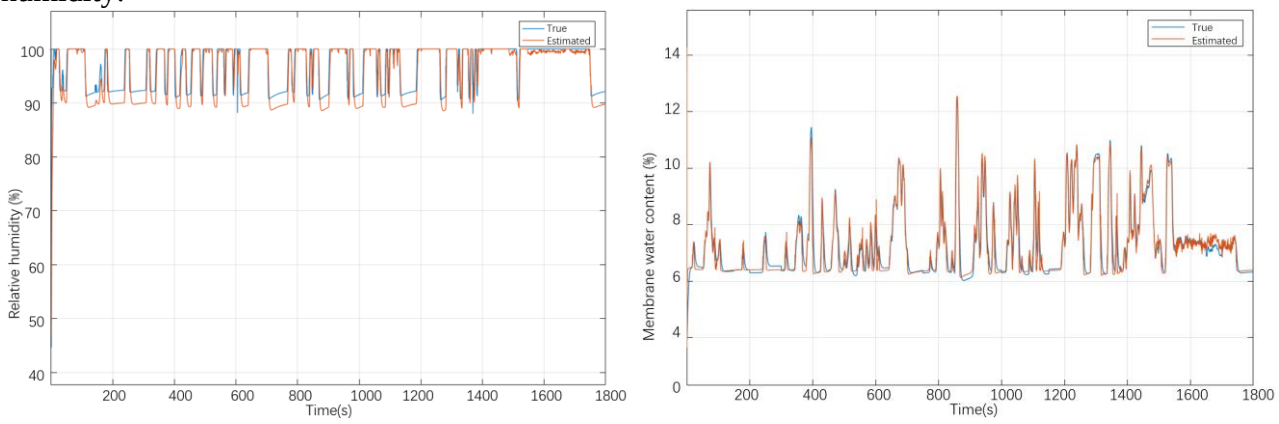

(a) (b)

Figure 7: Estimated vs. real humidity (a) and membrane water content (b) in the 70 kW stack.

As shown in Fig. 7, in the 70 kW stack, due to the use of exhaust gas to humidify the cathode inlet air, the inlet humidity sometimes becomes excessively high under the CWTVC operating condition, causing the stack's internal humidity to reach 100%. At this point, the cathode inside the stack is flooded. However, throughout the entire operating condition, the trend of the estimated humidity from the humidity observer closely matches that of the actual humidity obtained through the mechanistic model.

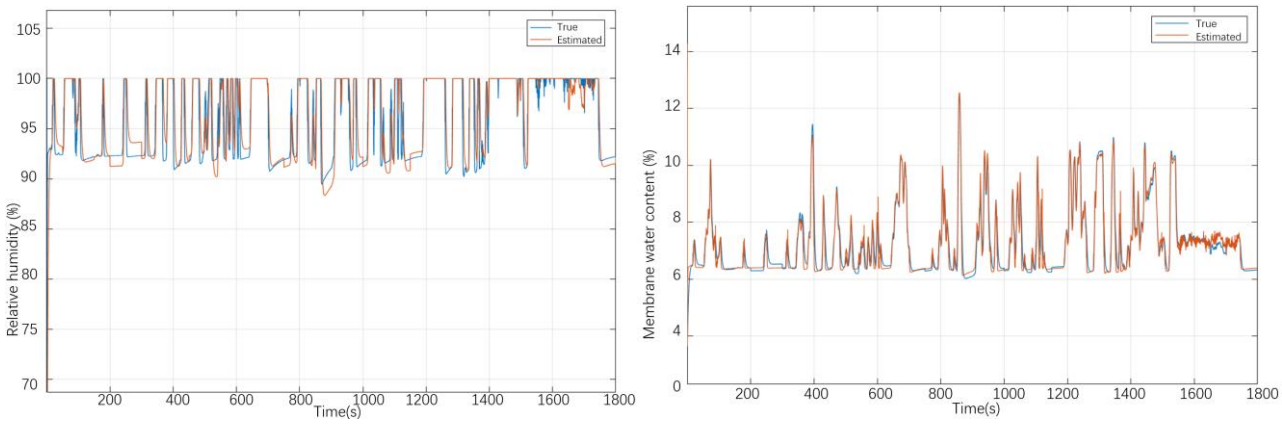

(a) (b)

Figure 8: Estimated vs. real humidity (a) and membrane water content (b) in the 120 kW stack.

As shown in Fig. 8, the performance of the 120 kW stack is similar to that of the previous two stacks. Overall, the humidity observer provides good estimation performance.

5. Conclusion

Membrane water content is a key factor influencing the efficiency and lifespan of PEMFC. Since it cannot be directly measured, this paper proposes a humidity observation algorithm to estimate it. First, by analysing the influencing factors of humidity, the necessary system inputs, states, and outputs for constructing a state observer were determined. Then, the system was identified in segments, and the input-output relationships as well as the state transition matrices for different operating conditions were obtained.

Subsequently, the system's observability was verified to ensure the feasibility of using a full-order state observer. A feedback matrix G was designed to ensure that the estimated states converge to the actual states over time. An incremental humidity state observer was then established in Simulink, and its accuracy was validated under the CWTVC working condition.

The experimental results show that, for the vast majority of the time, the estimated humidity values from the observer closely follow the trend of the actual humidity calculated using a physics-based model. This indicates that the humidity estimation algorithm has high reliability. Only when the stack current reaches a switching threshold, causing the observer to switch its internal model, does a transient deviation in the estimated humidity occur. Moreover, the observer performs well across stacks with power ratings of 20 kW, 70 kW, and 120 kW, demonstrating its good generalizability.

In summary, the proposed humidity estimation algorithm can effectively estimate the humidity within the fuel cell system and offers practical value. It provides reliable data support for the monitoring and control of fuel cell operating conditions.

References

[1] Zhu, H. M. (2022) Modeling of PEMFC System and Control Strategy Based on Oxygen Excess Ratio [D]. Jilin: Jilin University.

[2] Liu, H., Zhang, J. and Wang, X. (2015) Effects of Membrane Hydration on the Performance of Proton Exchange Membrane Fuel Cells. Journal of Power Sources, 293, 324-333.

[3] Zhao, J., Tu, Z. and Chan, S.H. (2022) In-Situ Measurement of Humidity Distribution and Its Effect on the Performance of a Proton Exchange Membrane Fuel Cell. Energy, 239(Part D), 122270.

[4] Jiao, J. and Chen, F. (2022) Humidity Estimation of Vehicle Proton Exchange Membrane Fuel Cell under Variable Operating Temperature Based on Adaptive Sliding Mode Observation. Applied Energy, 313, 118779.

[5] Jian, Z.Y. and Chen, H. (2018) A Humidity Identification Method for Proton Exchange Membrane Fuel Cell Based

on Cuckoo Algorithm. Electronic Devices, 41(3), 679-683.
[6] Zhu, X.H. (2017) Application of IT2FLS Based on Cuckoo Search Algorithm in Soft Measurement of PEMFC Humidity. Journal of Shaanxi University of Science & Technology, 35(4), 168-172.
[7] Hu, J.M. (2017) Dynamic Modeling and State Estimation of Water Transport in Vehicle Proton Exchange Membrane Fuel Cells [D]. Beijing: Tsinghua University.
[8] Zhou, S., Zhang, G., Fan, L., Gao, J., & Pei, F. (2022). Scenario-oriented stacks allocation optimization for multi-stack fuel cell systems. Applied Energy, 308*, 118328.*
[9] Gao, J., Zhou, S., Lu, Y., et al. (2024) Simulation of a Novel Integrated Multi-Stack Fuel Cell System Based on a Double-Layer Multi-Objective Optimal Allocation Approach. Applied Sciences, 14(7), 2961.
[10] Yousefkhani, M.B., Ghadamian, H., Daneshvar, K., Alizadeh, N. and Rincon Troconis, B.C. (2020) Investigation of the Fuel Utilization Factor in PEM Fuel Cell Considering the Effect of Relative Humidity at the Cathode. Energies, 13(22), 6117.
[11] Shi, L. (2021) Research on Water and Thermal Management Control Methods for Vehicle Multi-Stack Fuel Cell Systems [D]. Shanghai: Tongji University.
[12] Yun, H., Zhao, Y., & Zhong, Z. (2010). SOC estimation of vehicle auxiliary power battery based on Luenberger state observer. China Mechanical Engineering, 21(20), 2505–2509.